Preparation of transparent Ce:YSAG ceramic and its optical properties

Tao Feng, JianLin Shi [*], Danyu Jiang

Shanghai Institute of Ceramics, Chinese Academy of Sciences, 1295 Ding-Xi Road, Shanghai 200050, China

Abstract

Fine Ce:YSAG ($Y_3Sc_xAl_{(5−x)}O_{12}$) powders have been prepared by a chemical combustion method, and Ce:YSAG transparent ceramics was obtained by sintering the powders in hydrogen atmosphere. As Sc_2O_3 was introduced into the Ce:YAG crystal lattice to partially replace Al, the lattice of YSAG expanded and the optical properties of Ce:YSAG transparent ceramics has greatly changed from that of Ce:YAG ceramics. In Ce:YSAG transparent ceramics, the concentration quenching effect is greatly reduced, and the emission intensity is remarkably enhanced in Ce:YSAG as compared to Ce:YAG ceramics.
© 2008 Published by Elsevier Ltd.

Keywords: Ce:YSAG; Transparent ceramics; Optical properties; Sintering; Powder preparation

1. Introduction

Ce^{3+} ions have two UV laser channels which are connected with their $4f^{N−1}$–$4f^N(5d^1$–$4f^1)$ electric dipole allowed transitions (band emission). To achieve this stimulated emission (SE) generation, the radiations of either KrF and ArF excimer lasers or quadrupled pulsed laser ($\lambda_p \approx 0.266\,\mu m$) of $Y_3Al_5O_{12}$:Nd^{3+} were used as pumping sources. The high-gain UV band associated with $5d^1 \rightarrow {}^2f_{5/2,7/2}$ channels allows the tuning of the laser frequency up to $4000\,cm^{−1}$, which enables several modern important applications ranging from the nanotechnology, medical fields to LIDAR atmospheric sensing.[1] Currently, people usually use the fluoride crystals as the base media for Ce^{3+} SE laser, but Ce^{3+}-doped oxides are also promising materials for obtaining $5d^1$–$4f^1$ UV laser action. It is quite possible that in some oxide crystals doped with Ce^{3+} ions featuring high transparency in the 4.5–6 μm spectral range, mid-IR SE generation can be excited at the wavelengths of inter-stark transitions in the laser scheme using UV pumping in ${}^2f_{7/2} \rightarrow {}^2f_{5/2}$ channel by the cascade generation principle, or excited within the possible $5d^1 \rightarrow {}^2f_{7/2} \rightarrow {}^2f_{5/2}$ laser scheme using $4f^1 \rightarrow 5d^1$ absorption bands.

Yttrium aluminum garnet (YAG) $Y_3Al_5O_{12}$ is a stable refractory material with good thermal–mechanical properties. It can resist high temperature and thermal-shock, and it is transparent over a wide spectral range (0.18–6 μm) which makes it a privileged host for luminescent applications. YAG crystal has a cubic phase within the *Ia-3d* space group. The oxygen ions form a three-dimensional structure in which three kinds of sites for metal ions exist: dodecahedral, octahedral and tetrahedral ones. Yttrium cations are located at dodecahedral site, and aluminum cations are at octahedral and tetrahedral sites. After being incorporated into the lattice, lanthanide dopants will be located at dodecahedral site. Other small dopants are located at the octahedral and tetrahedral sites depending on the ionic radius of the doped cations. Lanthanide-doped YAG can be used as solid-state laser material.

But there are still some difficulties in the fabrication of Ce-doped YAG single crystals. Monchamp[2] has reported that the effective segregation coefficient of Pr^{3+} ions in YAG single crystals fabricated by Czochralski method is near zero, which means that Pr^{3+} ions are almost impossible to dissolve into the lattice of YAG single crystals. Since the ionic radius of Ce^{3+} is larger than that of Pr^{3+} ions, so it will be even more difficult to fabricate Ce^{3+}-doped YAG single crystals, especially at high doping level.

At present the Ce:YAG single crystals are obtained mainly from the boules grown via the traditional RF-heated Czochralki method using an iridium crucible[3,4], however, like growing

---

Nd-doped YAG there may be some limitations for growing high-quality and large-sized Ce:YAG crystals using the CZ method. Zhao et al.[5] fabricated Ce:YAG single crystals by temperature gradient technique (TGT), in this way they fabricated 3 in. high Ce:YAG single crystals with a cerium content of 0.8 at.%. However, the Ce^{3+} concentration along the growth direction was varying and became higher and higher toward the crystal bottom, resulting in the uneven distribution of Ce^{3+} ions, which will, inevitably, affect its optical properties.

Zych[6–8] has investigated the optical properties of Ce^{3+}-doped YAG transparent ceramic materials. Solid-reaction method was used for the preparation of the YAG powders, and transparent Ce:YAG ceramics were fabricated by a vacuum-hot-pressing approach. However, similar to the situation for single crystal, the Ce^{3+} doping concentration in the ceramics is also not higher than 0.8 at.%, and such a doping level has been found the highest in literatures so far reported in YAG.

An alternative approach to dope more Ce^{3+} is to substitute for aluminum with elements of larger size than Al in YAG without changing the crystal structure. The larger ionic size will lead to the lattice expansion, in this way more Ce^{3+} ions can be accommodated in the lattice, as Ce^{3+} is apparently larger than Y^{3+} for which Ce^{3+} substitutes. Sc^{3+} has larger size than Al^{3+}, and therefore is selected to replace Al^{3+} in YAG. Sc_2O_3 has been reported to form a cubic solid solution $Y_3Sc_xAl_{(5-x)}O_{12}$ (YSAG). The former study shows that $Cr^{4+}:Y_3Sc_xAl_{(5-x)}O_{12}$ single crystals had much decreased quantum efficiency as compared with $Cr^{4+}:Y_3Al_5O_{12}$.[9,10] The fabrication of Nd(Eu):YSAG ceramics has also been explored.[11–14]

Here we report the successful fabrication of transparent Ce^{3+}-doped yttrium aluminum (scandium) garnet (Ce:YSAG) ceramics by a novel chemical route.

2. Experiment

2.1. Material preparation

Ce-doped YSAG powders were prepared with a chemical combustion method. $Y(NO_3)_3\cdot H_2O$, $Al(NO_3)_3\cdot 8H_2O$, $Ce(NO_3)_3\cdot 6H_2O$, ammonium triacetic acid (NTA), Sc_2O_3 was used as raw materials. Solutions were obtained by dissolving $Y(NO_3)_3\cdot H_2O$, $Al(NO_3)_3\cdot 8H_2O$ and $Ce(NO_3)_3\cdot 8H_2O$ in deionized water and Sc_2O_3 in nitrate acid. The mixed solutions containing Y^{3+}, Al^{3+}, Sc^{3+} and Ce^{3+} ion were prepared from the as-prepared solutions with appropriate volumes. A Ce:YSAG precursor solution with a molar ratio of (Y + Ce):(Al + Sc) = 3:5, in a glass beaker, was continuously stirred during heating at 85–90 °C on a hot plate, and an appropriate amount of NTA aqueous solution (NTA to metal ion ratio of 1) was added into the metal ion solution. The mixed solution slowly became viscous, and turned into gel, then was put into a furnace pre-heated at 500 °C for combustion. A tan-colored powder formed afterwards. The powder was then calcined at different temperatures for 2 h for XRD analysis. The size of prepared powder is around 50–100 nm measured by TEM. The prepared powders were cold pressed into disks ≈20 mm in diameter at 70 MPa, then cold isostatically pressed at 200 MPa. Specimens were then pre-

sintered at 1000 °C for 2 h in air to remove any residue organics introduced during molding operation. Finally specimens were sintered at 1800 °C for 6–12 h with a heating rate of 15 °C/min in dry H_2. The annealing process was conducted at 1200 °C for 4 h in air, then cooled down to room temperature in furnace.

Both Ce-doped YAG and YSAG ($Y_3Sc_{1.5}Al_{3.5}O_{12}$) ceramics were prepared. The doping levels of Ce in YAG/YSAG varied from 0.5–4 at.%.

2.2. Characterization of specimens

XRD patterns of the samples were recorded on D/MAX-2550V (Japan RIGAKU) with Cu $K\alpha_1$ radiation. Optical transmission spectra and absorption spectra were obtained on a UV 3101 PC spectrophotometer (Japan Shimadzu) in the wavelengths from 200 to 800 nm. The emission spectra and fluorescence lifetime were obtained using Fluorolog-3 (Jobin Yvon American) with a Hamamatsu R5509-72 (InP/InGaAs) detector, and the emission spectra were recorded from 350 to 750 nm.

3. Result and discussion

Fig. 1 displays the photographs of the hydrogen-sintered Ce:YSAG pellets. The sintered pellets are 10 mm in diameter and 1 mm in thickness. The Ce:YSAG powder produced in such way is highly sintering active, and it can be sintered to high transparency at 1800 °C without SiO_2 addition which was used as a sintering additive by Ikesue[15–17]. As hydrogen atom is small, it can easily diffuse through the lattice/boundary of the ceramic sintering body, and facilitate the removal of pores. As a result, it can significantly reduce the porosity which would cause the scattering of light in ceramic body. At the same time, it can reduce the Ce^{4+} ions to Ce^{3+} ions which we need. We have successfully fabricated transparent Ce:YSAG ceramics by this method. At the same time, the colors of samples change from greenish yellow for Ce^{3+} 0.5 at.% concentration to yellow at 4 at.% of Ce^{3+} concentration.

Fig. 2 is a SEM microstructure of sintered $Ce:Y_3Sc_{1.5}Al_{3.5}O_{12}$ transparent ceramics. From this figure, we can see that the materials are dense without evident pores in the sintered sample, and the microstructure is quite uniform. Most grains in the microstructure are around 10–20 μm.
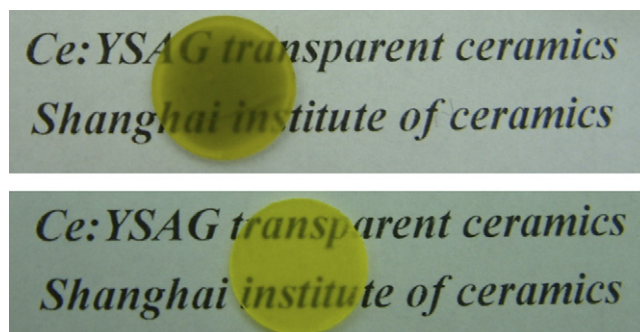

Fig. 1. Photographs of transparent Ce:YSAG pellet sintered under hydrogen atmosphere at 1750 °C for 6 h (a) Ce: 1 at.%; (B) Ce: 4 at.%.
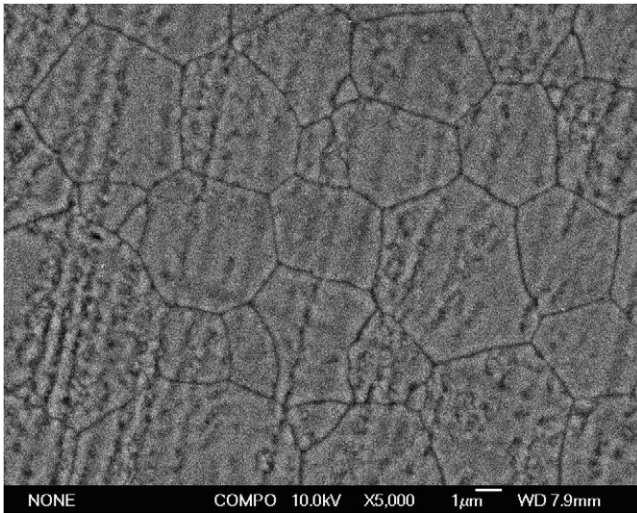
Fig. 2. SEM microstructure of sintered Ce:$Y_3Sc_{1.5}Al_{3.5}O_{12}$ transparent ceramics.

Fig. 4. XRD pattern of sintered Ce:$Y_3Sc_{1.5}Al_{3.5}O_{12}$ sample and the standard pattern of YAG.

Fig. 3 shows the in-line light transmission curve of Ce:$Y_3Sc_{1.5}Al_{3.5}O_{12}$ transparent ceramics and Ce:YAG single crystal. From this curve, we can see that the transmittance is higher than 60%, a little lower than that of Ce:YAG single crystal. This indicates that there is no apparent second phase in the body of Ce:$Y_3Sc_{1.5}Al_{3.5}O_{12}$ transparent ceramics. It also implies that the Ce and Sc ions have entered the YAG lattice, and do not exist as a single phase in the body of the transparent ceramics. From this figure, we also can see that the difference of absorption band between Ce:$Y_3Sc_{1.5}Al_{3.5}O_{12}$ transparent ceramic and Ce:YAG single crystal is apparent. It may be caused by the different concentrations of Ce doping in the materials (2 at.% in $Y_3Sc_{1.5}Al_{3.5}O_{12}$ transparent ceramics and 0.8 at.% in YAG single crystal, respectively) and the addition of Sc into the lattice of YAG.

The XRD patterns of sintered samples are presented in Fig. 4. It is clear that the samples have a pure cubic phase. The XRD patterns of Ce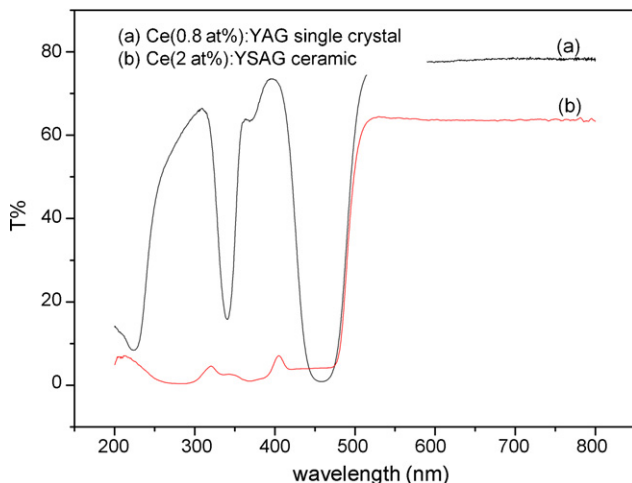:$Y_3Sc_{1.5}Al_{3.5}O_{12}$ are almost identical to that of pure YAG with a little shift of the peak positions towards smaller 2θ values (larger lattice constants) due to the substitution of scandium for aluminum, which means that the Ce and Sc ions have dissolved into the crystalline lattice and do not exist as a separate phase.

Fig. 5 presents the calculated[10] and measured YSAG lattice constant. We measured the lattice constant from the XRD patterns of samples with different level scandium substitutions for aluminum. It can be seen that the data difference between the calculated and measured is apparent, though not large. As the substitution level of scandium for aluminum increases, the lattice constant of YSAG become larger and lattice experiences significant expansion.

The transmittance spectra of Ce:$Y_3Sc_{1.5}Al_{3.5}O_{12}$ transparent ceramic with different concentrations of Ce^{3+} were shown in Fig. 6. In this figure, we can see that as the Ce^{3+} concentration increases in Ce:$Y_3Sc_{1.5}Al_{3.5}O_{12}$, the absorption peak becomes wider. When the Ce^{3+} concentration increases to 4 at.%, almost all light at wavelengths below 480 nm can be absorbed, which

Fig. 3. Light transmission curve of 2 at.% Ce:$Y_3Sc_{1.5}Al_{3.5}O_{12}$ transparent ceramics and 0.8 at.% Ce:YAG single crystal.
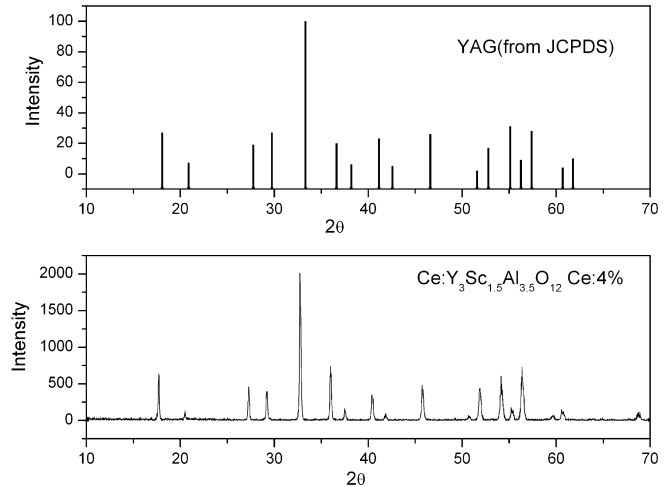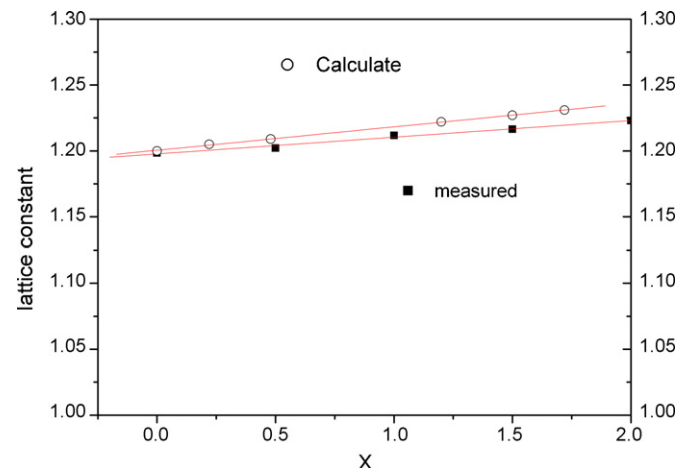

Fig. 5. The calculated and measured lattice constants of $Y_3Sc_xAl_{5-x}O_{12}$ as a function of x value in $Y_3Sc_xAl_{5-x}O_{12}$.
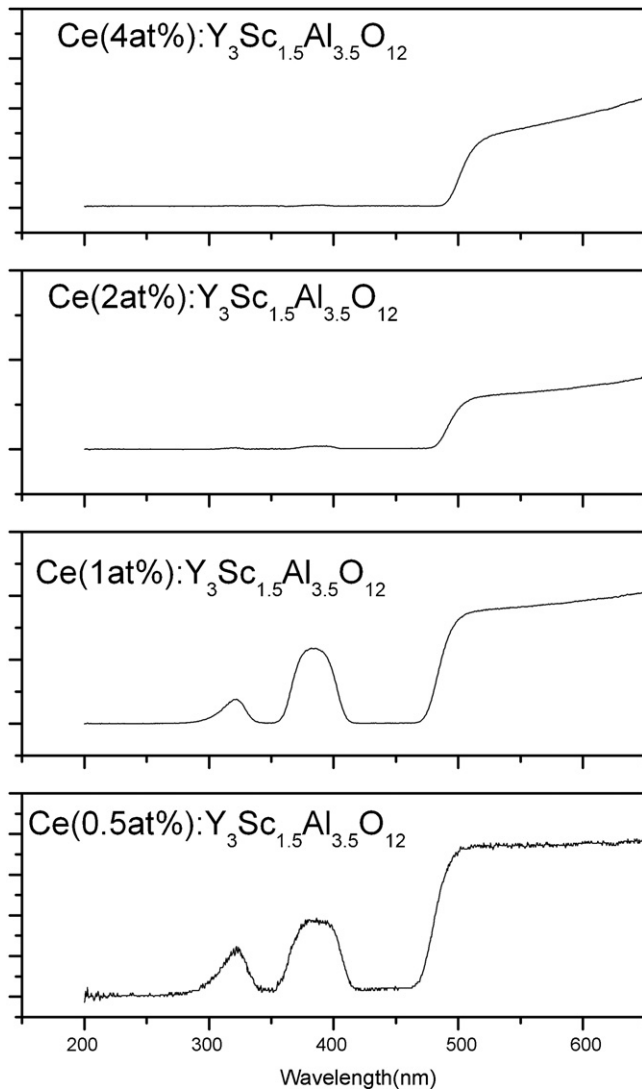
Fig. 6. Light transmission curve of Ce:$Y_3Sc_{1.5}Al_{3.5}O_{12}$ transparent ceramics at different Ce^{3+} doping levels.

Fig. 7. Emission spectra of (a) Ce:$Y_3Sc_{1.5}Al_{3.5}O_{12}$ and (b) Ce:YAG ceramics with different concentrations of Ce^{3+} (excited at 460 nm).

means that the energy level has been changed by doping Ce^{3+} with increased concentrations.

Emission spectra of Ce:$Y_3Sc_{1.5}Al_{3.5}O_{12}$ and Ce:YAG with different concentrations of Ce^{3+} are presented in Fig. 7. From this figure, we see there exist some differences in the emission spectra between Ce:$Y_3Sc_{1.5}Al_{3.5}O_{12}$ and Ce:YAG. As the Ce^{3+} concentration increases to 4 at.% in Ce:$Y_3Sc_{1.5}Al_{3.5}O_{12}$, the emission intensity increases to a much higher level than those with lower Ce^{3+} concentration. That is to say, when Ce^{3+} concentration is as higher as 4 at.% in YSAG, there is still no evident concentration quenching. However in Ce:YAG ceramics, the overall emission intensity is much lower than those of Ce:YSAG, and moreover, the highest emission intensity was obtained at 0.8 at.% of Ce^{3+} doping level, and beyond the concentration the emission intensity begins to decrease significantly. This implies that the Sc substitution for Al in YAG ceramics is very effective in suppressing the concentration quenching effect of the radiative rare-earth ions and enhancing the light emission intensity due to the lattice expansion effect of YSAG by Sc ions.
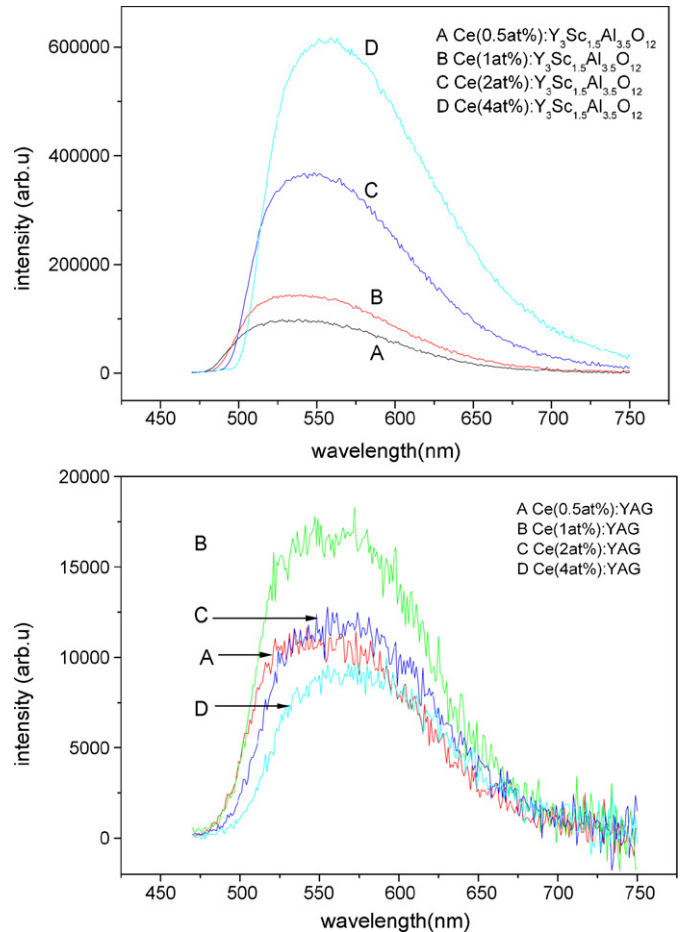
4. Conclusion

We have fabricated Ce:YSAG and Ce:YAG transparent ceramics by sintering the fine powders derived by a chemical combustion method in hydrogen atmosphere. The Sc substitution for Al apparently causes the lattice expansion of YSAG. As the Ce concentration increases beyond 2 at.%, the Ce:YSAG shows near complete absorption for lights at wavelengths below 480 nm. The Ce:YSAG transparent ceramics show remarkably enhanced light emission intensity and much suppressed concentration quenching effect than those of Ce:YAG ceramics at the same Ce doping levels.

References

1. Sarukura, N., Dubinskii, M. A., liu, Z., Semashko, V. V., Naumov, A. K., Korableva, S. L. *et al.*, *IEEE J. Sel. Top. Quantum Electron.*, 1995, **1**, 792.
2. Monchamp, R. R., The distribution coefficient of neodymium and lutetium in Czochralski grown $Y_3Al_5O_{12}$. *J. Cryst. Growth*, 1971, **11**, 310–312.
3. Ludziejewski, T., Moszunski, M., Kapusta, M., Wolski, D., Klamra, W., Moszynska, K. *et al.*, *Nucl. Instrm. Methods A*, 1997, **398**, 287.
4. Chao-hong, H., Lei, L., Dong-fang, Z., Qing-hai, Q., Yun-kui, L., Shao-tang, Y. *et al.*, *J. Synth. Cryst.*, 2001, **30**, 354 [in Chinese].
5. Zhao, G. J., Zeng, X. H., Xu, J., Xu, Y. Q. and Zhou, Y. Z., Characteristic of large-sized Ce:YAG scintillation crystal grown by temperature gradient technique. *J. Cryst. Growth*, 2003, **253**, 290–296.

6. Zych, E., Brecher, C. and Wojtowicz, A. J., Luminescence properties of Ce-activated YAG optical ceramic scintillator materials. *J. Lumin.*, 1997, **75**, 193–203.

7. Zych, E., Brecher, C. and Lingertat, H., Host-associated luminescence from YAG optical ceramics under gamma and optical excition. *J. Lumin.*, 1998, **78**, 121–134.

8. Zych, E. and Brecher, C., Temperature dependence of Ce-emission kinetic in YAG:Ce optical ceramic. *J. Alloy Compd.*, 2000, **300–301**, 495–499.

9. Kück, S., Petermann, K., Pohlmann, V. and Huber, G., Near-infrared emission of Cr^{4+}-doped garnets: lifetimes, quantum efficiencies and emission cross sections. *Phys. Rev. B: Condens. Matter.*, 1995, **51**, 17323–17331.

10. Kück, S., Petermann, K., Pohlmann, U., Schönhoff, U. and Huber, G., Tunable room-temperature laser action of Cr^{4+}-doped $Y_3Sc_xAl_{5-x}O_{12}$. *Appl. Phys. B*, 1994, **58**, 153–156.

11. Sato, Y., Taira, T. and Ikesue, A., Spectral parameters of Nd^{3+}-ion in the polycrystalline solid solution composed of $Y_3Al_5O_{12}$ and $Y_3Sc_2Al_3O_{12}$. *Jpn. J. Appl. Phys.*, 2003, **42**, 5071–5074.

12. Tao, F., Shi, J. and Jiang, D., Fluorescence emission enhancement of transparent Nd:YSAG ceramics by Sc_2O_3 doping. *J. Opt. Soc. Am. B.*, 2005, **22**(10), 2134–2137.

13. Tao, F., Shi, J. and Jiang, D., Synthesis and greatly enhanced fluorescence of transparent Nd:YSAG ceramic. *J. Mater. Res.*, 2005, **20**(9), 2322.

14. Tao, F., Shi, J. and Jiang, D., Preparation and optical properties of transparent Eu^{3+}:$Y_3Al_{5(1-x)}Sc_{5x}O_{12}$ ceramics. *J. Am. Ceram. Soc.*, 2006, **89**, 1590–1593.

15. Ikesue, A., Furusateo, I. and Kamata, K., Fabrication of polycrystalline, transparent YAG ceramics by a solid-state reaction method. *J. Am. Ceram. Soc.*, 1995, **78**, 225–228.

16. Ikesue, A. and Kamata, K., Microstructure and optical properties of hot isostatically pressed Nd:YAG Ceramics. *J. Am. Ceram. Soc.*, 1996, **79**, 1927–1933.

17. Ikesue, A., Yoshida, K. and Kamata, K., Transparent Cr^{4+}-doped YAG ceramics for tunable lasers. *J. Am. Ceram. Soc.*, 1996, **79**, 507–509.